International Journal of Heat and Mass Transfer 55 (2012) 4987–4995

Contents lists available at SciVerse ScienceDirect

International Journal of Heat and Mass Transfer

journal homepage: www.elsevier.com/locate/ijhmt

Heat transfer characteristics during subcooled flow boiling of a kerosene kind hydrocarbon fuel in a 1 mm diameter channel

Zhaohui Liu, Qincheng Bi *, Yong Guo, Qianhua Su

State Key Laboratory of Multiphase Flow in Power Engineering, Xi'an Jiaotong University, Xi'an 710049, PR China

ARTICLE INFO

Article history:
Received 10 October 2011
Received in revised form 20 April 2012
Accepted 21 April 2012
Available online 15 June 2012

Keywords:
Hydrocarbon fuel
Subcooled flow boiling
Heat transfer
Mini-channel

ABSTRACT

The subcooled flow boiling heat transfer characteristics of a kerosene kind hydrocarbon fuel were investigated in an electrically heated horizontal tube with an inner diameter of 1.0 mm, in the range of heat flux: 20–1500 kW/m^2, fluid temperature: 25–400 °C, mass flux: 1260–2160 kg/m^2 s, and pressure: 0.25–2.5 MPa. It was proposed that nucleate boiling heat transfer mechanism is dominant, as the heat transfer performance is dependent on heat flux imposed on the channel, rather than the fuel flow rate. It was found that the wall temperatures along the test section kept constant during the fully developed subcooled boiling (FDSB) of the non-azeotropic hydrocarbon fuel. After the onset of nucleate boiling, the temperature differences between inner wall and bulk fluid begin to decrease with the increase of heat flux. Experimental results show that the complicated boiling heat transfer behavior of hydrocarbon fuel is profoundly affected by the pressure and heat flux, especially by fuel subcooling. A correlation of heat transfer coefficients varying with heat fluxes and fuel subcooling was curve fitted. Excellent agreement is obtained between the predicted values and the experimental data.

1. Introduction

The heat transfer characteristics in micro- and mini-channel have been the focus of intense research activities in the past decades due to the development of biology technology, fuel cell, electronic equipment cooling, and aviation applications. Previous investigations were mostly concentrated on the water and refrigerants [1–22]. In this paper, a kerosene kind hydrocarbon fuel was investigated. It is very important to research on the heat transfer characteristics of hydrocarbon fuel in the field of thermal management of the aerospace vehicles [23–28].

Endothermal hydrocarbon fuel is used as a coolant in the regenerative cooled scramjet engines [23], where the cooling structure is made up of mini-channels. Investigation on heat transfer characteristics of hydrocarbon fuel in mini-channels is basic for the design of cooling structure. The high heat flux encountered (about 1 MW/m^2) results that boiling heat transfer inevitably takes place. Heat transfer processes with boiling are one of the most complex transport phenomena in the field of heat and mass transfer [1]. So many complexities [29,30] are included in these processes, such as nonlinearity, instabilities, transition to turbulence, and two phase phenomena resulting from nucleation, such as the growth and motion of the bubbles along the surface of the heater, and the complex dynamic and kinetic interactions between the two phases of the fluid, and between the two phases and the solid surface of the heater. The various involved parameters are so complex that the real physics of the process is to a great extent not well understood as yet [1].

Flow boiling heat transfer is characterized by drastically different flow regimes for different mass fluxes. Two different flow regimes [2] are described for the low and high mass velocity separately. Subcooled film boiling, is a kind of departure from nucleate boiling (DNB), would occur more at high mass velocity and short tube.

Previous studies [2–4] showed that very high CHF could be attained with subcooled flow boiling of water at high mass velocities in small diameter tubes. Mudawar and Bowers [2] reported that the subcooled film boiling could occur instead of the dryout deterioration at higher mass flux, higher entrance subcooling, higher heat flux and lower L/D in tubes with D = 0.33–2.67 mm.

The dominant heat transfer mechanism inside a micro- or mini-channel remains an open question. A summary of the previous relevant studies had been achieved by Lee and Mudawar [4]. For the nucleate boiling, the local heat transfer coefficient is dependent on heat flux, but not mass flux, density or quality [5–7]. For the film evaporation [8–11], the heat transfer coefficient is a function of mass flux [30]. Pressure is also an important parameter in boiling heat transfer. A number of literatures [7,9,12,13] reported that the heat transfer for nucleate boiling was enhanced with pressure increasing, but opposite results [10] also had been attained that the pressure had little or negative effect to the boiling heat transfer.

* Corresponding author. Tel.: +86 029 82665287; fax: +86 029 82665287.
E-mail address: qcbi@mail.xjtu.edu.cn (Q. Bi).

0017-9310/$ - see front matter © 2012 Elsevier Ltd. All rights reserved.
http://dx.doi.org/10.1016/j.ijheatmasstransfer.2012.04.039

Nomenclature

D	diameter (m)
L	length (m)
T	temperature (°C)
P	pressure (MPa)
U	voltage (V)
I	electricity current (A)
G	mass flux (kg/m^2 s)
q	heat flux (kW/m^2)
m	mass flow rate (kg/s)
h	heat transfer coefficient (kW/m^2 °C)
Q_m	heat sink (kJ/kg)
λ	thermal conductivity (W/m °C)
μ	viscosity (Pa s)
L_i	the distance of the thermocouple i away from the front electrode (m)
ΔT	temperature difference (°C)
ΔT_{sat}	wall superheat, $\Delta T_{sat} = T_w - T_{sat}$ (°C)
ΔT_{sub}	liquid subcooling, $\Delta T_{sub} = T_{sat} - T_b$ (°C)
η	heat efficiency
Re	Reynolds number, $Re = GD/\mu$

Subscripts

w	wall
b	bulk
loc	local
in	inside of channel
out	outside of channel
sat	saturation
sub	subcooling

Table 1
Special features of present study.

Features	Characteristics
Channel	A single circular tube with inner diameter of 1.0 mm
Heat flux	20–1500 kW/m^2
Heating mode	Electrically heated
Mass flux	1260, 1680 and 2100 kg/m^2 s
Pressure	0.25–3.0 MPa
Fluid temperature	25.0–400.0 °C
Working fluid	A kerosene kind hydrocarbon fuel

The boiling mechanism in this paper might be much different and more complicated than the studies reported before, as the working fluid used here was an organic mixture without azeotropic behavior. It is well known that the boiling temperature keeps constant for an azeotropic mixture same as a pure substance, but increases for a non-azeotropic mixture at a given pressure.

The subject of this paper was to investigate the heat transfer processes of a hydrocarbon fuel passing through a uniformly heated mini-channel. Table 1 lists the special features of the present study. It is a primary goal of the paper to develop a fundamental understanding of the flow boiling heat transfer for a non-azeotropic mixture. More attentions were paid to the correlations of heat transfer coefficient with heat flux, fluid temperature, mass flux and pressure. Comparisons of the heat transfer coefficient with the existing correlations were conducted. A new correlation was developed for the heat transfer coefficient with fuel subcooling, which is an important factor in the subcooled flow boiling of hydrocarbon fuel.

2. Experimental setup and hydrocarbon fuel

Fig. 1 is a schematic figure of the experimental system. Hydrocarbon fuel was driven by a triplex plunger pump to flow through the test system. The mass flow rate of hydrocarbon fuel was measured at the inlet by a Coriolis mass flow meter 9. The pressure was measured at the outlet of test tube by Rosemount pressure transducer 12. The mass flow and pressure of the test system were regulated precisely by a series of Swagelok needle valves (7, 8, 15, 16) respectively.

An electrically heated GH3128 high temperature nickel alloy tube (heated length, 245 mm; inner diameter, 1.0 mm; wall thickness, 0.5 mm) was used as test section, as shown in Fig. 2. The average roughness value of tube surface (Ra) was 0.821 μm, measured by Roughness Measuring Instrument TR300. There is a tube length of 40 mm not heated at each end of the tube to avoid the flow entrance effect and stabilize the fluid flow.

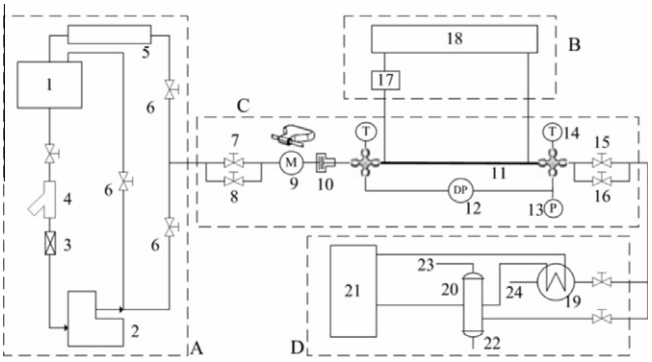

Fig. 1. Schematic figure of experimental system. 1. Fuel tank. 2. Triplex plunger pump. 3. Expansion joint. 4. Filter. 5. Cooling section. 6. Valve. 7, 8 Swagelok valve. 9. Mass flow rate density. 10. Electricity insulating joint. 11. Test tube. 12. Pressure transducer. 13. Differential pressure transducer. 14. K-type sheathed thermocouple. 15, 16. High temperature valve. 17. AC current transformer. 18. Power supply. 19, 20. Cooling structure. 21. Water cooler. 22. Liquid sample collection. 23. Gas sample collection. 24. Fuel exit.

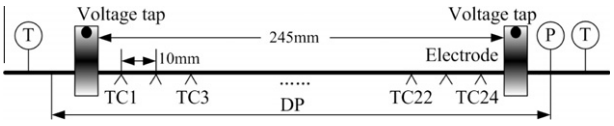

Fig. 2. Schematic figure of test section.

In order to measure the local outside wall temperature, 24 K-type thermocouples (TC) were spot welded on the outside surface of the horizontal tube with a 10 mm uniform space between each other. The fluid temperature was measured in the inlet and outlet of the test tube with K-type sheathed thermocouple of 1.0 mm outside diameter. The test tube was covered with thermal insulation fiber to avoid heat losses, and also to guarantee the accuracy of the wall temperature measurement.

2.1. Properties of hydrocarbon fuel tested

The hydrocarbon fuel studied is a kind of kerosene, which is made up of a blend of hydrocarbons, with cycloalkanes

30.50 wt.%, alkanes 20.06 wt.% and aromatics 49.42 wt.%. The average molecular formula is $C_{11.9}H_{23.4}$. Fuel density is 838.0 kg/m^3 at the condition of 25 °C and atmosphere pressure. The Engler distillation curve of the fuel was measured with the onset of distillation at 196.0 °C, and 10 wt.% distillated at 206.0 °C, 90 wt.% at 243.0 °C, and 100% at 258.0 °C at atmosphere pressure.

The thermal physical properties of hydrocarbon fuel are mostly referred from Hu [24], which include the temperature dependent viscosity, density and saturation pressure. The fuel's critical pressure and critical temperature are about 2.5 MPa and 400 °C respectively which are consistent with the critical properties of general kerosene hydrocarbons in the previous review by Edwards and Zabarnick [25].

The hydrocarbon fuel after tested was analyzed by GC, and it was found that chemical reaction will not take place until the fluid temperature achieved approximately 500 °C at the test condition. As a result, that the heat transfer behaviors companioned with chemical reaction are not included in this paper.

3. Data reduction

The local heat transfer coefficient at each portion of the test section containing a thermocouple (TC) was calculated.

The local heat transfer coefficient h_{loc} is given as

$$h_{\mathrm{loc}} = q_{\mathrm{loc}}/(T_{w,in} - T_b) \tag{1}$$

The local heat flux q_{loc} was calculated as follows:

$$q_{\mathrm{loc}} = UI\eta/\pi D_{in}L \tag{2}$$

A heat efficiency correlation of η with $T_{w,\mathrm{out}}$ was measured by the heat balance method. The Joule heat generated from the electricity power was balanced with the heat loss to the ambience when no working fluid was employed in the tube.

Heat flux density imposed is nearly uniform along the electrically heated tube. Because the heat loss differs along the tube due to the different wall temperature, the heat flux absorbed by the fluid along the tube would always be more or less different from each other. However, the statistical discrepancy along the tube is less than 5.0% of the total heat flux.

The local fluid temperature T_b at each TC point was calculated from the corresponding heat sink of hydrocarbon fuel. A third order polynomial function of heat sink Q_m with T_b is shown in Eq. (4), which was fitted from the experimental data with fuel temperature ranging from 50.0 °C to 300.0 °C. The local heat sink was derived by Eq. (4)

$$Q_m = 0.8 + 1.0T_b + 4.9\times10^{-3}T_b^2 - 4.3\times10^{-6}T_b^3 \tag{3}$$

$$Q_m = \frac{UI\eta}{1000m}\frac{L_i}{L} \tag{4}$$

The coolant side wall temperature at each thermocouple position was determined by deducting the calculated temperature drop through the wall, seen in Eq. (5) referred from [14]

$$T_{w,in} = T_{w,\mathrm{out}} - \frac{D_{in}}{2}\frac{q_{\mathrm{loc}}}{\lambda_{\mathrm{loc}}}\left[\frac{D_{\mathrm{out}}^2}{D_{\mathrm{out}}^2 - D_{in}^2}\ln\frac{D_{\mathrm{out}}}{D_{in}} - \frac{1}{2}\right] \tag{5}$$

Table 2
Uncertainties of experimental measurement.

Parameters	Uncertainty
Temperature, T (°C)	±1.0
Pressure, P (MPa)	±0.04
Mass flux, G (%)	±1.2
Heat flux, q (%)	±2.1
Heat transfer coefficient, h (%)	±4.1

All the experimental Uncertainties were evaluated in Table 2. Uncertainty of the heat transfer coefficient was 4.1%.

4. Results and discussion

The high subcooled liquid fuel with temperature of about 25 °C entered the test channel with mass fluxes of about 1260, 1680 or 2100 kg/m^2 s. The outlet fluid temperatures ranged from 25 °C to about 400 °C, which were achieved by different heat fluxes imposed on the test tube. Pressure at the outlet was fixed at a given value from atmosphere pressure to 3.0 MPa. As a result, the heat transfer performance with different pressures, mass fluxes, fluid temperatures and heat fluxes could be attained.

4.1. The interesting wall temperature

Boiling heat transfer capitalizes on latent heat exchange, which both increases the convective heat transfer coefficient during the fluid flow and helps maintain a more uniform device surface temperature, dictated mostly by the coolant's saturation temperature for the pure substances like water or the azeotropic mixtures like refrigerant. The almost uniform wall temperature increases with the heat flux increasing [5,11,14].

4.1.1. The wall temperature at different heat fluxes and fuel mass flow rates

In the paper, an interesting and significant phenomenon noticed is that the wall temperatures keep constant along the channel during the subcooled flow boiling of the non-azeotropic hydrocarbon fuel, which was similar to the boiling of pure compounds and the azeotropic ones [7] with a constant boiling temperature at a constant pressure, but the boiling temperature of hydrocarbon fuel increases with quality distillated.

Fig. 3 shows the variation of local inner wall temperatures with fluid temperatures for different heat fluxes, in which a curve at a constant heat flux represents a wall temperature profile along the whole test channel with 24 TC points. The outlet fuel temperature described by the last point of each curve is dependent on the heat flux imposed on the test channel due to the same L/D of 245 and the same mass flux of 1680 kg/m^2 s.

The wall temperature profiles can be obviously separated to three parts according to the almost non-change wall temperature value of about 320.0 °C along the test channel. Simply the three parts are below, nearly equal to and above the constant temperature value of 320.0 °C respectively. The wall temperatures at the 1st TC point when different heat fluxes imposed at a given mass

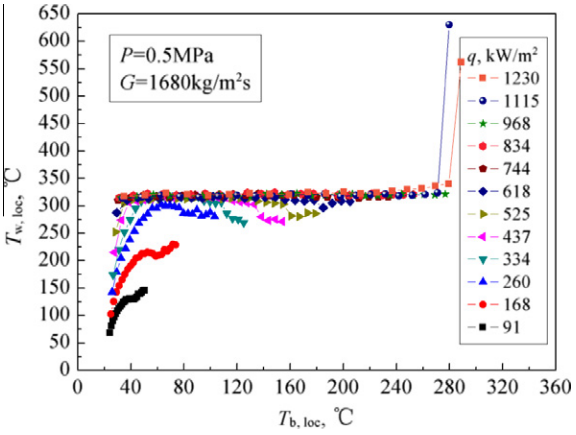

Fig. 3. The coolant side wall temperatures with local bulk fluid temperatures for different heat fluxes.

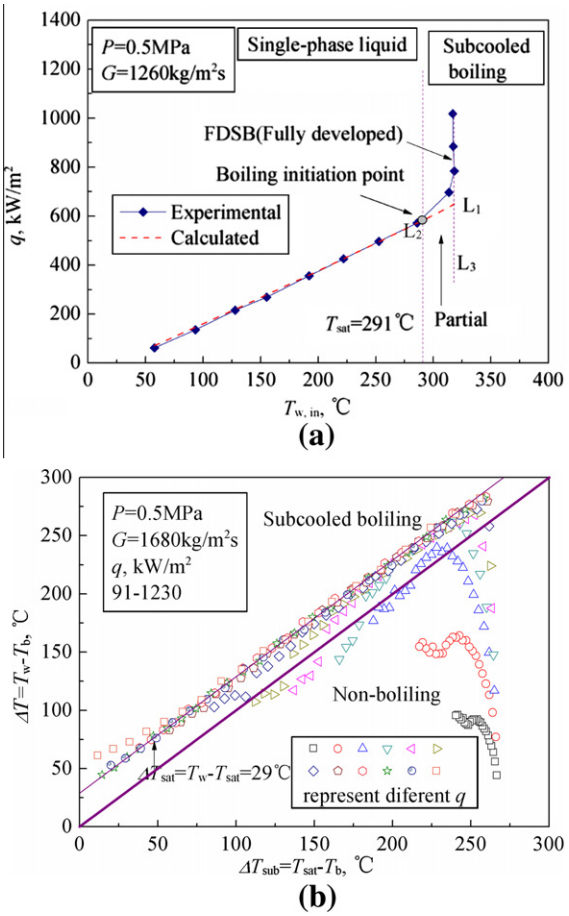

Fig. 4. Different heat transfer modes changes as heat flux increased. (a) Boiling curve at the first TC point of test tube near the inlet. (b) Temperature difference between surface and fuel vs. fuel subcooling.

flow rate and inlet subcooling ($T_{b,in}$ = 25 °C) are individually described in Fig. 4(a) to demonstrate the heat transfer mode experienced.

Two key temperatures play significant roles here, the saturation temperature T_{sat} and the fully developed subcooled boiling (FDSB) wall temperature T_{FDSB}, about 291.0 °C and 320.0 °C respectively at 0.5 MPa. As the heat flux increases the heat transfer mode passes through the single phase non-boiling, the partial subcooled boiling, and the fully developed subcooled nucleate boiling.

At fuel temperature below saturation, the wall temperature increases with heat flux according to the single phase relationships [29]. The Dittus-Boelter relation was rewritten to predict the heat flux of forced convection [15], shown in Eq. (6). Good agreement was achieved between the experiment data and predicted ones, shown in Fig. 4(a). When the wall temperature becomes larger than the saturation temperature, the nucleation commences, and the partial boiling occurs until the wall temperature approached to about 320.0 °C, and then the fully developed nucleation boiling took it place, in which case the wall temperature becomes independent of bulk fuel temperature, seen in Fig. 3. The heat transfer mode at all TC points can be illustrated in Fig. 4(b). The diagonal of equality between $(T_w - T_b)$ divided the boiling and non-boiling region.

$$q_{cal} = 0.023 Re_b^{0.8} Pr_b^{0.4} \lambda (T_w - T_b)/D_{in} \quad (6)$$

When the wall temperature deviated from the FDSB region to rise quickly, the heat transfer deterioration happened. It was supposed that film boiling happened, as the fuel temperatures at points of deterioration were still less or much less than the saturation temperature of fuel at the test pressure.

4.1.2. The wall temperature at different pressures

Pressure would always play a significant role when evaporation or boiling occurs as a result of the performance of phase change [5,7,12,13]. It was found that the uniform wall temperatures of FDSB along the channel are profoundly affected by the different outlet pressures. Fig. 5 shows the variation of the inner wall temperatures with local fluid temperatures for different pressures at q = 640 kW/m^2 and G = 1680 kg/m^2 s.

The wall temperatures were almost uniform along the whole channel at pressures from 0.25 MPa to 0.49 MPa, which demonstrated that the FDSB occurred in the whole channel length. As the pressure increased to above 0.8 MPa, the heat transfer mode was partially pushed back to the single phase non-boiling region, as the wall temperature at the entrance of channel departed from the $T_{w,FDSB}$ to be values even lower than the T_{sat}. It was indicated that the subcooled boiling was suppressed by the increased pressure at the entrance, and a larger heat flux was needed to motivate it.

As the pressure increased to 1.13 MPa, the wall temperature at the outlet of the channel also departed from the FDSB region, which was also noticed in Fig. 3 at heat fluxes from 334 to 525 kW/m^2 at 0.5 MPa. However, the mechanism contributed to the departure near tube outlet was somewhat different from the single phase liquid flow at the entrance. In addition to saturation temperature increases due to the pressure increase, the flow transition to turbulent is another reason for it. A detail explanation will be performed in the following part.

The function of fuel saturation temperature T_{sat} with saturation pressures P_{sat} is shown in Eq. (7). It found that the averaged FDSB wall temperature T_w profile deeply correlated with the saturation temperature.

$$P_{sat} = 0.012 - 1.082 \times 10^{-3} T_{sat} + 1.792 \times 10^{-5} T_{sat}^2 - 9.843 \times 10^{-8} T_{sat}^3 + 2.461 \times 10^{-10} T_{sat}^4 \quad (7)$$

A correlation of the T_w of FDSB with pressures fitted by a third stage polynomial is shown in Eq. (8), and the heat transfer coefficient of FDSB can be calculated by the Eq. (9). The local pressures were considered as the pressures measured at the channel outlet. Because the pressure drops of hydrocarbon fuel were less than 20.0 kPa at all test conditions. So the difference of local pressures along the test tube, which were much less than outlet pressure, could be neglected. A comparison of the measured heat transfer coefficient h_{exp} with the calculated values h_{cal} was conducted at pressures from 0.25 MPa to 2.5 MPa. It resulted that deviations of all the 123 points at FDSB region were in 5.0%.

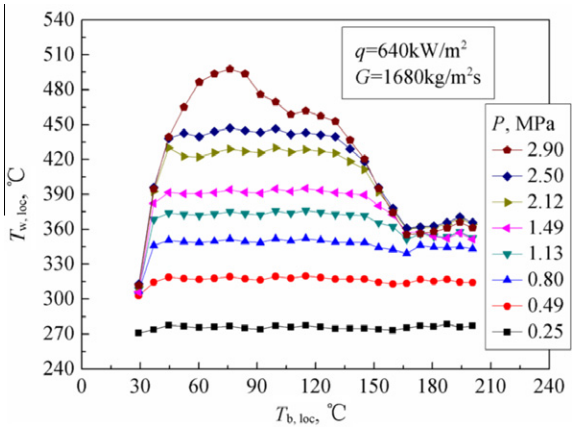

Fig. 5. Pressure effect on the inner wall temperature.

$$T_{w,\mathrm{FDSB}} = a_0 + a_1 P + a_2 P^2 + a_3 P^3$$
$$a_0 = 229.44, \quad a_1 = 208.22, \quad a_2 = -91.49, \quad a_3 = 17.06 \tag{8}$$

$$h_{\mathrm{FDSB}} = q/(T_{w,\mathrm{FDSB}} - T_b) \tag{9}$$

As the wall temperature analyzed above, it concluded that larger heat flux and lower pressure were more beneficial to motivate the FDSB in the tube to produce an almost uniform wall temperature profile.

4.2. Fluid flow regimes and heat transfer mechanisms

Variation of local heat transfer coefficients, wall temperatures and bulk fluid temperatures with heat fluxes at the last TC point near the outlet are shown in Fig. 6 at $P = 0.5$ MPa, $G = 1260$ kg/m^2 s. Once the FDSB occurred, the wall temperature almost hardly changed with heat fluxes until the heat transfer deterioration happened, and then the wall temperature quickly rising up to 600.6 °C from 327.6 °C. A correlation of the superheated temperatures ΔT_{sat} ($\Delta T_{\mathrm{sat}} = T_w - T_{\mathrm{sat}}$) hardly increasing with heat fluxes is shown in Fig. 7(a). As mentioned above that the superheat temperatures $\Delta T_{\mathrm{sat}} > 0$ represented the nucleation commencing and the onset of partial boiling. Comparison of the measured data with correlations from Jens and Lottes [16] (shown in Eq. (10)) and Thom et al. [14] (shown in Eq. (11)) were presented. It indicated that the deviation between the experimental data and the predicted ones from Jens and Lottes mostly did not exceed 25.0%, shown in Fig. 7(b).

$$\Delta T_{\mathrm{sat}} = 25 q^{0.25} \exp(p/62), \quad p\text{-}bar, \quad q\text{-MW/m}^2 \tag{10}$$

$$\Delta T_{\mathrm{sat}} = 22.65 q^{0.5} \exp(p/87), \quad p\text{-}bar, \quad q\text{-MW/m}^2 \tag{11}$$

The equation of incipient boiling curve given by Bergles and Rohsenow [17] (shown in (12)) is also shown in Fig. 7. All the experimental data was at the right side of the predictive curve

$$(\Delta T_{\mathrm{sat}})_{\mathrm{ONB}} = 0.556 \left(\frac{q}{1082 P^{1.156}} \right)^{0.436 P^{0.0234}}, \quad q\text{-W/m}^2, \quad P\text{-}bar \tag{12}$$

Kandlikar [20] reported that three heat transfer regions in the subcooled boiling had been identified by earlier investigators as partial boiling, fully developed boiling (FDB), significant void flow (SVF) region. Once the wall temperature exceeds the saturation temperature, boiling can be initiated. When the single-phase liquid convective heat transfer become insignificant, the FDB is established. Subsequently, the mean wall temperature keeps almost constant in the FDB region.

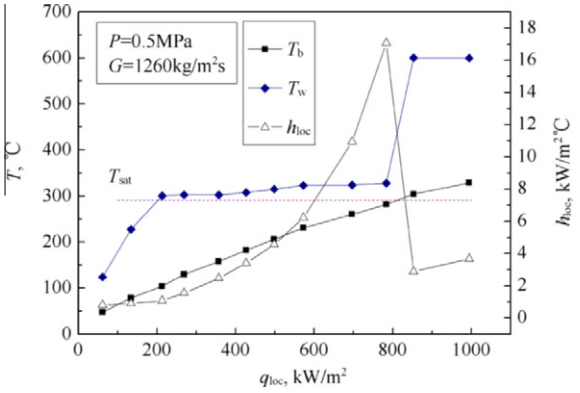

Fig. 6. Local heat transfer coefficients, wall temperatures and bulk fluid temperatures with heat fluxes at the last TC point near the outlet.

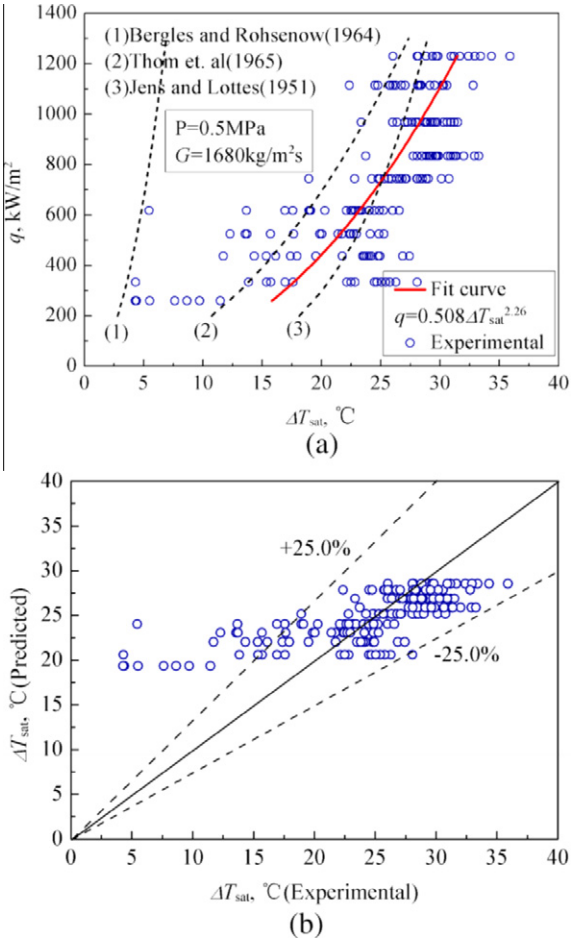

Fig. 7. (a) Boiling curve with heat fluxes vs. wall superheat ΔT_{sat} for all the measured data with $\Delta T_{\mathrm{sat}} > 0$. (b) Comparision of the measured data with the one predicted by Jens and Lottes [16].

Results indicated that subcooled nucleation boiling occurred for several reasons. That the wall temperature departs from the single-phase liquid line L_1 to increase faster shown in Fig. 4 means the onset of nucleation, which was also indicated by the wall temperature equaling to the fuel saturation temperature at the departure point. That the uniform wall temperature was independent of mass flux and bulk fluid temperature (a reflection of fuel subcooling) and only a function of pressure, demonstrated that the fully developed subcooled nucleation boiling occurred.

It was noticed that the uniform heat flux and uniform wall temperature happened simultaneously at the boiling condition. So the heat transfer coefficient is simply inverse proportion to the bulk fluid temperature according to the Newton cooling formula, see in Eqs. (1) and (9). The only thing was to ensure the FDSB occurring and the values of pressure in the test tube on which the FDSB wall temperature was dependent.

Actually the wall temperature of FDSB was strongly dependent on the saturation temperature at respective pressure as be shown in Fig. 9(b).

The flow regimes in the test channel are very clear now according to the analysis above. It can be obviously seen in Fig. 4 that all the fuel temperatures were less than the saturation temperature at FDSB region. The heat transfer mode was separated from FDSB at the high heat flux region, where the subcooled film boiling deterioration happened, and the film boiling would gradually move to the foreside of test tube with higher fuel subcooling due to the increasing heat flux imposed, seen in Fig. 3.

4.3. Effect of pressure on heat transfer performance

As analyzed above, pressure is the most crucial parameter in the process of FDSB. And it is the parameter the wall temperature of FDSB mainly depending on.

Fig. 8(a) shows the heat transfer performance at $G = 1680\ \mathrm{kg/m^2\,s}$ for different test pressures, in which both single-phase liquid flow and two-phase boiling heat transfer are included. The heat transfer coefficients were nearly the same at different pressures at $q < 170\ \mathrm{kW/m^2}$, which was as a result of the average temperature differential between the inner wall and fluid temperature almost independent of pressure.

The unique characteristic of the different heat transfer modes were clearly described by the trend of heat flux with temperature difference $T_w - T_b$. That the temperature difference $T_w - T_b$ increased with heat flux represented the single-phase liquid flow region. The subcooled boiling commenced when the temperature difference began to decrease with heat flux increasing.

The averaged superheat and uncertainties at FDSB region with different pressures are shown in Fig. 8(b). The heat transfer performance was compared with relation of Jens and Lottes [16]. The superheat needed to motivate boiling increased with pressure increasing. It indicated that the subcooled boiling was suppressed by the increasing pressure.

An attempt was tried to get the mechanism of pressure on the boiling heat transfer. Fig. 9(a) shows the heat transfer coefficients with bulk fuel temperatures for different test pressures at FDSB region. The heat transfer coefficient was strongly correlated with the fuel subcooling ΔT_{sub}, shown in Fig. 9(b). A beautiful curve was fitted as Eq. (13), and the deviations of all the 123 data with the prediction values by the fitted equation are in 7.0%.

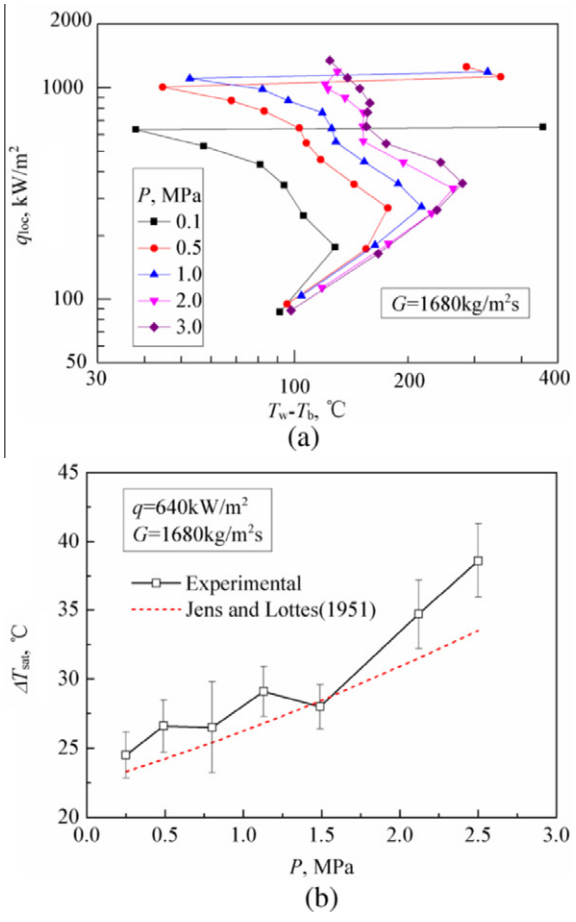

Fig. 8. Heat transfer performance at $G = 1680\ \mathrm{kg/m^2\,s}$ for different test pressures. (a) Boiling curve of local heat flux with temperature difference $T_w - T_b$ at the last TC point. (b) Comparison of the experimental superheat with others' correlation.

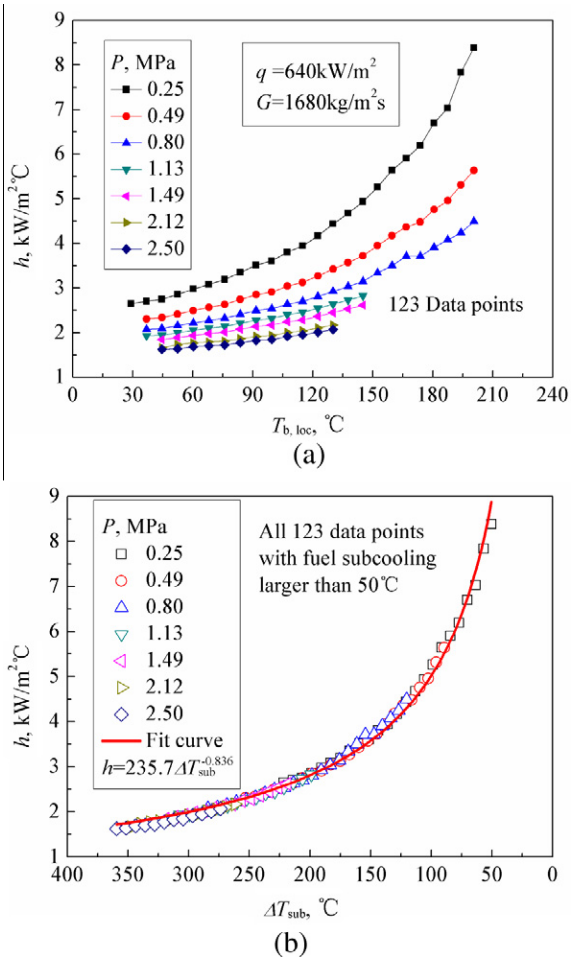

Fig. 9. Heat transfer coefficients with (a) bulk fuel temperatures and (b) fuel subcooling ΔT_{sub} for different test pressures at FDSB region.

$$h = 235.7\Delta T_{sub}^{-0.836}$$
$$0.25\ \mathrm{MPa} < P < 2.5\ \mathrm{MPa},\ 50\ ^\circ\mathrm{C} < \Delta T_{sub} < 370\ ^\circ\mathrm{C} \qquad (13)$$

By considering the fuel subcooling ΔT_{sub} as horizontal ordinate, the heat transfer coefficients were immerged into one curve at different pressures. It strongly indicates that the fuel subcooling is the key effect of heat transfer. At the same fuel temperature, the saturation temperature T_{sat} increases with pressure increasing, and the fuel subcooling increases. The heat transfer coefficient decreases with fuel subcooling increasing. As a result, the nucleation is suppressed by pressure increase.

The analysis of pressure effect on subcooled boiling here is much different from the previous literatures [9,12]. It reported that the heat transfer strengthened at higher pressure for saturated nucleate boiling, which was based on the same quality of working fluid.

A number of literatures [1,4,7,12,14,18] have reported the strong correlation between liquid subcooling and the boiling heat transfer performance. In general, the heat transfer is enhanced by liquid subcooling decreasing. Bao et al. [7] reported that the heat transfer coefficient decreased with pressure increasing at the same location of test channel with the same heat flux and mass flux at subcooled boiling condition. The nucleation of subcooled fluid with the same temperature was suppressed at higher pressure, which caused the heat transfer coefficient reduced at the same fluid temperature.

The boiling heat transfer was always described by the superheat in others' work. Moreover, the subcooling was used to character

the heat transfer of hydrocarbon fuel in this paper. A strong correlation was found between the heat transfer and the fuel subcooling.

4.4. Heat transfer coefficients at different mass fluxes, heat fluxes, and bulk fuel temperatures

Fig. 10 shows the variation of local heat transfer coefficients with local bulk fluid temperatures at FDSB region for different mass fluxes and heat fluxes. It can be obviously seen that the profiles are divided into three groups according to the three given heat flux series. In every group the mass fluxes of 1260, 1680 and 2100 kg/m^2 s are covered. Results indicated that the local heat transfer coefficients were independent of mass fluxes at the heat flux from 644 to 1050 kW/m^2 under nucleate boiling condition. The heat transfer coefficient increased with fluid temperature increasing as a result of the fuel subcooling decreased.

A correlation of heat transfer coefficients with heat fluxes at FDSB region was fitted in Fig. 11(b), with the original data covering a wide range of heat transfer coefficients from 1.0 to 11.0 kW/m^2 °C at a given heat flux, shown in Fig. 11(a). The fitted correlation is shown by Eq. (14)

$$h = 0.33\Delta T_{sub}^{-0.836}(q + 37.3) \quad (14)$$

Comparison of the measured heat transfer coefficients with the predicted values from Eq. (14) is shown in Fig. 12. Deviations of almost all points are in 10.0% at all the operation conditions, and the RMS error is 3.9%. Earlier investigates [1,14,18,19] also reported that the heat transfer of nucleate boiling increased with heat flux increasing, but which were not so obviously occurred in our experiments.

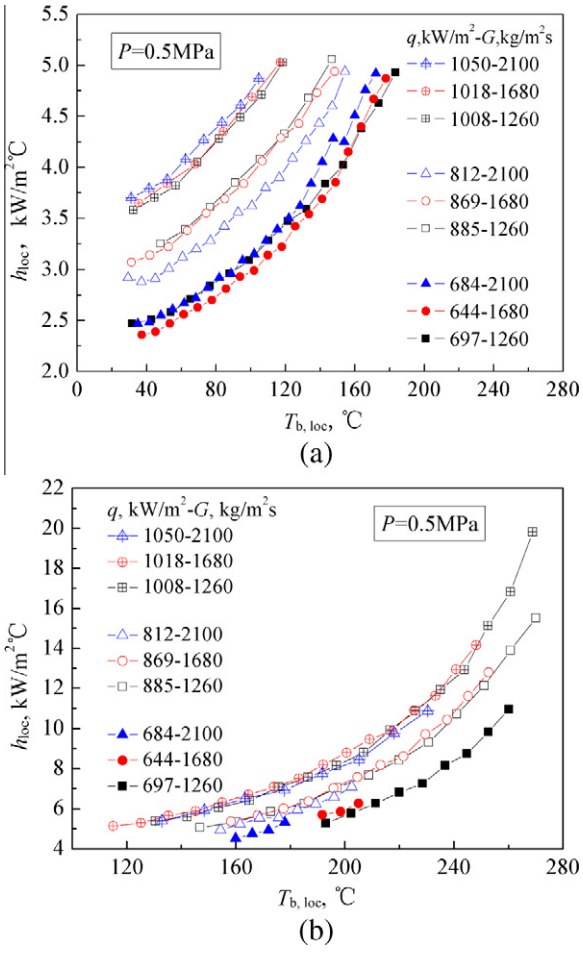

Fig. 10. Comparison of local heat transfer coefficients with local bulk fluid temperatures T_b at different heat fluxes and velocities. (a) Low T_b region. (b) High T_b region.

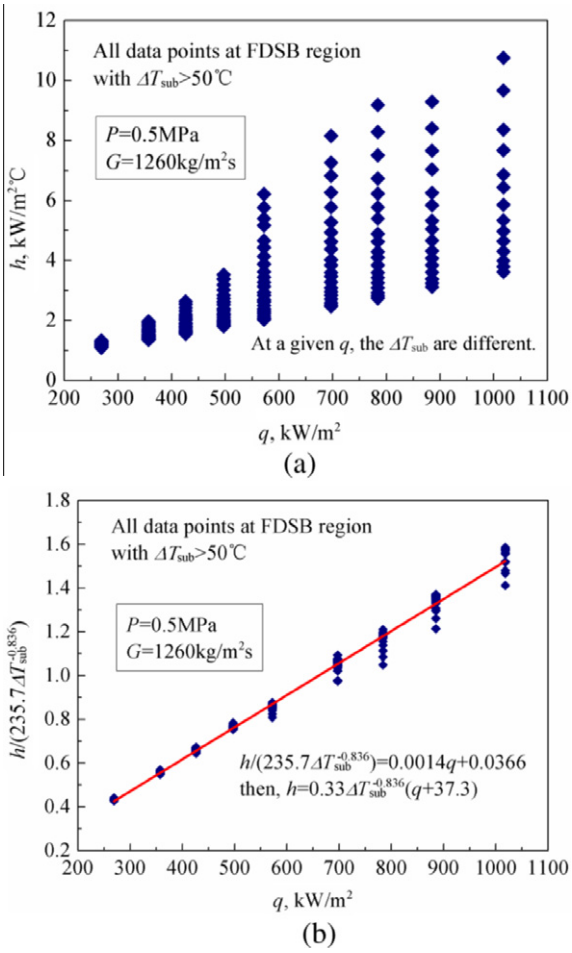

Fig. 11. Local heat transfer coefficients with heat fluxes at FDSB region. (a) The original data. (b) The deduced data and the curve fitted.

4.5. A valuable problem to solve

As mentioned above, the wall temperature deviated from the FDSB region at the conditions with low heat fluxes or high pres-

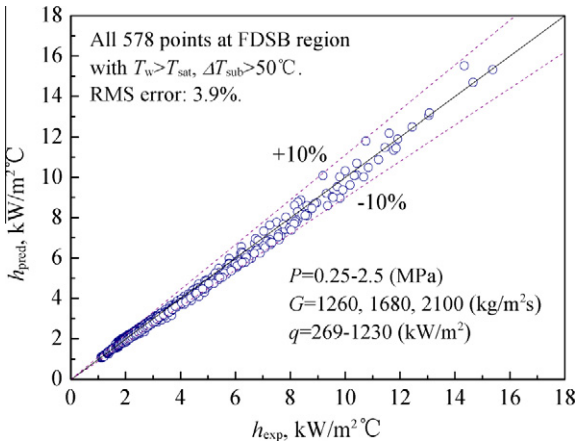

Fig. 12. Comparison of the measured heat transfer coefficients with the predicted values by the fitted curve at all the operation conditions.

sures see in Figs. 3 and 5. At the FDSB condition, the heat transfer near the outlet would experience a process including three stages according to the increasing heat fluxes imposed. First, the wall temperature decreased to below the constant temperature of FDSB at low heat fluxes. And then with heat flux increasing the wall temperature increased to be equal to the constant wall temperature. At last, the wall temperature rose up quickly at high heat flux conditions due to heat transfer deterioration. It indicated that at the first stage higher heat flux or less pressure was necessary to approach the FDSB region.

The heat transfer coefficients with *Re* for $G = 1680\ kg/m^2\ s$ at the conditions of the first stage are shown in Fig. 13. Supposing that the FDSB occurred in the whole tube length, the suppositional h_{loc} is also shown as the hollow patterns. The actual h_{loc} near the outlet of the tube begin to deviate from the FDSB region to increase faster at $Re \approx 2600$ and $q = 334\ kW/m^2$. With heat flux increasing the *Re* of deviation points increased.

Experiment measurement attained that the flow pattern transited to turbulence at $Re \approx 2500$, and the laminar flow happened at $Re < 1600$ in the 1 mm inner diameter tube with the hydrocarbon fuel. The hydrocarbon fuel passed through laminar flow, transition flow and turbulence flow with fuel temperature increasing from inlet temperature of 25 °C to above 150 °C in the tube.

Fluid flow transition to turbulence occurred when fluid temperature was 88 °C at $G = 1680\ kg/m^2\ s$, 114 °C at $G = 1260\ kg/m^2\ s$. The transition points were also consistent with the wall temperature deviation points near the outlet of the tube in Fig. 3. As the flow pattern transited to turbulence, the effect of forced convection fluid velocity and Reynolds number became important. It was found that larger velocity leading to much more wall temperature decreasing from the FDSB region. As Reynolds number increases up to turbulence value, the curves of heat transfer coefficients with various heat fluxes are merged into one curve in Fig. 13. It indicated that turbulence became vigorous, and the effect of heat flux disappeared. As our knowledge it has not been reported in previous literature, which is the inverse process of nucleation with curves of heat transfer for different fluid velocities merging into one curve dependent on heat flux, see in literatures [19,20].

The fluid can be divided into two parts due to the large temperature gradient in the test tube. One part is the bulk fluid which is the single phase liquid flow at the center axis of the tube, and the other part is the fluid near the inner surface of the tube with bubble flow.

The heat transfer behavior is the co-action of the single phase liquid flow at the central part and the nucleate boiling surrounding it. The heat transfer is enhanced when the bulk fluid flow transfers to turbulence. It is shown that the wall temperature departed from the FDSB region to a value below the saturation temperature near the outlet of the tube, the nucleation was fully suppressed by the heat transfer enhancement as a result of the turbulence, seen much clearly in Fig. 3. When the heat transfer mode is turbulence dominant, the heat transfer coefficient will linearly increasing with *Re*, see in Fig. 13. However, the effect of turbulence will decrease due to the enhanced nucleation with the heat flux increasing.

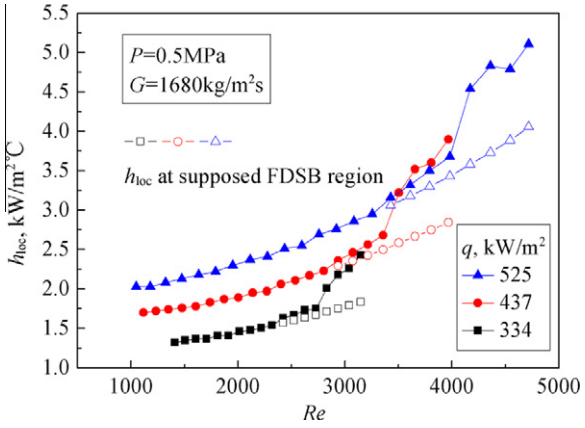

Fig. 13. The heat transfer coefficients with *Re* at the boiling conditions wherein the wall temperature deviates the FDSB region near the outlet of test tube.

5. Summary

The subcooled flow boiling and heat transfer behavior in a uniformly heated mini-channel with an inner diameter of 1.0 mm were investigated using a kerosene kind hydrocarbon fuel as working fluid. The major findings are summarized as follows.

(1) The nucleate boiling heat transfer was dominant during subcooled flow boiling of the non-azeotropic hydrocarbon fuel, and it was enhanced with heat flux increasing and independent of the mass flow rate.
(2) During the fully developed subcooled boiling (FDSB), the wall temperature kept almost constant along the channel, and was independent of bulk fluid temperature and fuel flow rate. However, it was profoundly affected by the pressure in the channel. Adding heat flux would slowly increase the wall temperature of FDSB.
(3) The fuel subcooling was found affecting the heat transfer of hydrocarbon fuel strongly. The boiling heat transfer at same fluid temperature was suppressed due to the increase of subcooling as pressure increasing. Higher heat transfer coefficient was attained at higher fuel temperature owing to the fuel subcooling decrease. In order to predict the heat transfer coefficients at FDSB region for different pressures, heat fluxes, and fluid temperatures, a correlation of heat transfer coefficient h with fuel subcooling ΔT_{sub} and heat flux q was curve fitted. Excellent agreement was obtained between the predicted data and the experimental data.
(4) The hydrocarbon fuel experiences an evolution from laminar flow, transition flow to turbulence flow as fuel temperature increasing in the channel. A combined action of the forced convective flow and the nucleation was observed. The flow transition to turbulence would enhance the heat transfer performance, as a result, the nucleation was suppressed and the wall temperature decreased. Higher heat flux and lower pressure were expected to facilitate the heat transfer mode to approach the FDSB region.

Further investigations are necessary to determine the boundary of the FDSB region. It will be a much more interesting thing to discover the difference heat transfer mechanism of hydrocarbon fuel at high subcooled, low subcooled and saturated boiling. To our knowledge, few investigations were reported related to the FDSB of a mixture including multi-components with a wide range of boiling temperatures in previous literatures. It is significant to uncover the mechanism of the flow boiling of non-azeotropy mixtures.

References

[1] J. Straub, Boiling heat transfer and bubble dynamics in microgravity, Adv. Heat Transfer 35 (2001) 57–168.
[2] I. Mudawar, M.B. Bowers, Ultra-high critical heat flux (CHF) for subcooled water flow boiling-I: CHF data and parametric effects for small diameter tubes, Int. J. Heat Mass Transfer 42 (8) (1999) 1405–1428.
[3] D.D. Hall, I. Mudawar, Ultra-high critical heat flux (CHF) for subcooled water flow boiling-II: high-CHF database and design equations, Int. J. Heat Mass Transfer 42 (8) (1999) 1429–1456.

[4] J. Lee, I. Mudawar, Two-phase flow in high heat-flux micro-channel heat sink for refrigeration cooling applications: Part II-heat transfer characteristics, Int. J. Heat Mass Transfer 48 (5) (2005) 941–955.
[5] Y. Sun, L. Zhang, et al., Subcooled flow boiling heat transfer from microporous surfaces in a small channel, Int. J. Therm. Sci. 50 (6) (2011) 881–889.
[6] M.W. Wambsganss, D.M. France, J.A. Jendrzejczyk, T.N. Tran, Boiling heat transfer in a horizontal small-diameter tube, J. Heat Transfer 115 (4) (1993) 963–972.
[7] Z.Y. Bao, D.F. Fletcher, B.S. Haynes, Flow boiling heat transfer of Freon R11 and HFCFC123 in narrow passages, Int. J. Heat Mass Transfer 43 (18) (2000) 3347–3358.
[8] S. Lin, P.A. Kew, K. Cornwell, Two-phase heat transfer to a refrigerant in a 1 mm diameter tube, Int. J. Refrig. 24 (1) (2001) 51–56.
[9] X. Huo, L. Chen, Y.S. Tian, T.G. Karayiannis, Flow boiling and flow regimes in small diameter tubes, Appl. Therm. Eng. 24 (8–9) (2004) 1225–1239.
[10] Y.Y. Hsieh, T.F. Lin, Saturated flow boiling heat transfer and pressure drop of refrigerant R-410A in a vertical plate heat exchanger, Int. J. Heat Mass Transfer 45 (5) (2002) 1033–1044.
[11] A.B. Helali, Effects of water contamination on sub-cooled flow boiling heat transfer, Energy Convers. Manage. 52 (5) (2011) 2288–2295.
[12] J.R. Thome, Boiling in microchannels: a review of experiment and theory, Int. J. Heat Fluid Flow 25 (2) (2004) 128–139.
[13] A. Greco, G.P. Vanoli, Flow boiling heat transfer with HFC mixtures in a smooth horizontal tube, Part I: Experimental investigations, Exp. Thermal Fluid Sci. 29 (2) (2005) 189–198.
[14] J.R.S. Thom, W.M. Walker, et al., Boiling in subcooled water during flow up heated tubes or annuli, Proc. Inst. Mech. Eng. 180 (1966) 226–246.
[15] T. Sato, H. Matsumura, On the conditions of incipient subcooled-boiling with forced convection, Bull. JSME 7 (26) (1964) 392–398.
[16] W.H. Jens, P.A. Lottes, An analysis of heat transfer, burnout, pressure drop, and density data for high pressure water, Argonne Natl. Lab, Report No. ANL-4627-1951.
[17] A.E. Bergles, W.M. Rohsenow, The determination of forced convection surface-boiling heat transfer, ASME J. Heat transfer 86 (1964) 365–372.
[18] K. Hata, S. Masuzaki, Subcooled boiling heat transfer for turbulent flow of water in a short vertical tube, J. Heat Transfer 132 (1) (2010) 011501.
[19] T. Harirchian, S.V. Garimella, Effects of channel dimension, heat flux, and mass flux on flow boiling regimes in microchannels, Int. J. Multiph. Flow 35 (4) (2009) 349–362.
[20] S.G. Kandlikar, Heat transfer characteristics in partial boiling, fully developed boiling, and significant void flow regions of subcooled flow boiling, J. Heat Transfer-ASME 120 (1998) 395–401.
[21] K. Suzuki, A. Oshima, et al., Subcooled flow boiling in a minichannel, Heat Transfer Eng. 32 (7–8) (2011) 667–672.
[22] J.Y. Shin, M.S. Kim, et al., Experimental study on forced convective boiling heat transfer of pure refrigerants and refrigerant mixtures in a horizontal tube, Int. J. Refrig. 20 (4) (1997) 267–275.
[23] T. Edwards, USAF supercritical hydrocarbon fuels interests, AIAA 1993-0807, 1993.
[24] Z.H. Hu, Experimental Investigation on Heat transfer characteristics of kerosene used in rocket engine, Master's thesis, Xi'an Jiaotong University, Xi'an, 1996.
[25] T. Edwards, S. Zabarnick, Supercritical fuel deposition mechanisms, Ind. Eng. Chem. Res. 32 (12) (1993) 3117–3122.
[26] L.L. Diane, L.M. Michael, Evaluation of heat transfer and thermal stability of supercritical JP-7 fuel, AIAA 1997-3041, 1997.
[27] C.B. Matthew, Thermal stability and heat transfer characteristics of RP-2, AIAA 2008-5126, 2008.
[28] Z.H. Hu, T.K. Chen, et al., Heat transfer to kerosene at supercritical in small-diameter tube with large heat flux, J. Chem. Ind. Eng. (China) 53 (2) (2002) 134–138.
[29] D. Butterworth, G.F. Hewitt, Two-phase Flow and Heat Transfer, Oxford University Press, Oxford, 1977. pp. 204–212.
[30] J.H. Lienhard IV, J.H. Llenhard V, A Heat Transfer Textbook, third ed., Prentice Hall, New Jersey, 2006. pp. 496–505.